

First-order dielectric susceptibilities of tetrahedrally coordinated semiconductors

J. N. Decarpigny and M. Lannoo

Laboratoire de Physique des Solides, Institut Supérieur d'Electronique du Nord, 3 rue François Baës, 59046 Lille Cedex, France*

(Received 21 April 1975)

This work describes the computation of the first-order dielectric susceptibilities of tetrahedrally coordinated semiconductors, within a molecular model. It allows the discussion of several approximations which have been frequently used in the study of second-order dielectric susceptibilities and the estimation of local-field effects. First of all, it is shown that the accuracy of a bonding-antibonding model decreases with increasing ionicity. Secondly, using a method of moments and a model curve for the $\epsilon_2(E)$ spectrum, reasonable values of the low-energy threshold of $\epsilon_2(E)$ as well as of the average dielectric gap defined by Phillips are obtained. Then local-field effects are estimated. A Lorentz-Lorenz correction seems to be valid, if one includes the drastic reduction due to self-polarization effects. Finally, the separation of the contributions of bond charge and charge transfer to $\epsilon_1(0)$ is discussed.

INTRODUCTION

Recently, there has been great interest in the theoretical evaluation of linear and nonlinear dielectric susceptibilities of tetrahedrally coordinated semiconductors. First-principles calculations are possible¹⁻³ but they involve difficult computations which imply a loss of physical insight. Thus, numerous models have been developed. The susceptibilities have been determined from transitions between bonding and antibonding states,⁴⁻⁷ from the computation of the average values of given operators in the ground state,⁸⁻¹⁰ and from a bond-charge model¹¹ or a charge-transfer model.¹² In general, the parameters which are required are fitted to the first-order susceptibility, and then the model is applied to higher-order susceptibilities. Particularly, this allows the inclusion of local-field effects without any attempt to determine them.

Our aim is to do a critical analysis of these models, by the direct computation of the first-order susceptibility $\epsilon_1(0)$ and an estimation of the local-field effects. For this, we elaborate a linear-combination-of-atomic-orbitals (LCAO) description of the ground state, following a "molecular model" which gives correct predictions for many physical properties. We first analyze the bonding-antibonding model and show that its accuracy decreases with increasing ionicity. Then, using a method of moments, a computation is achieved which gives reasonable results and allows a determination of local-field effects with a formalism first described by Wisner,¹³ in the tight-binding limit.

In Sec. I, the molecular model is developed based upon the assumption that bonds between nearest neighbors do not interact.^{6,7,14-16} In order to obtain a reasonable description of the electronic charge density, the overlap between atomic sp^3 hybrid orbitals from which bonds are built up is

included. Ionicity parameters are determined within this model. In Sec. II, the static dielectric constant $\epsilon_1(0)$ is computed, in terms of transitions between bonding and antibonding molecular states. We show that this method includes the results of Harrison's bond-orbital model^{6,7} and we demonstrate that the f -sum rule is not verified in the case of the most-ionic compounds. Then, the computation of $\epsilon_1(0)$ is developed, starting with the evaluation of the first moments of $\epsilon_2(E)$, the imaginary part of the energy-dependent dielectric function. This computation only requires a LCAO description of the ground state. The general method is given in Sec. III, its application to the molecular model being achieved in Sec. IV. We show that the low-energy threshold of the $\epsilon_2(E)$ spectrum can be reasonably determined, as well as the average dielectric gap defined by Phillips.¹⁷ Finally, local-field effects are estimated. A Lorentz-Lorenz correction seems to be valid, if one takes account of the drastic reduction due to the influence of the self-polarization.

I. MOLECULAR MODEL; DESCRIPTION OF THE GROUND STATE

We consider tetrahedrally coordinated crystals of the $A^N B^{8-N}$ type, where N is equal to 4, 5, or 6. In these crystals, each A atom is surrounded by four B atoms and vice versa. The molecular orbitals for each bond AB are built out of atomic sp^3 hybrid orbitals φ_a and φ_b pointing towards each other (Fig. 1). In the molecular, or bond-orbital, approximation^{6,7,14-16} only the following matrix elements of the Hamiltonian H are taken into account:

$$\alpha_a = \langle \varphi_a | H | \varphi_a \rangle, \quad \alpha_b = \langle \varphi_b | H | \varphi_b \rangle, \quad \beta = \langle \varphi_a | H | \varphi_b \rangle. \quad (1.1)$$

α_a and α_b are intra-atomic terms and β is a resonance integral. The sp^3 orbitals are then coupled by pairs, leading to a set of diatomic molecules with a bonding level E_B and an antibonding level

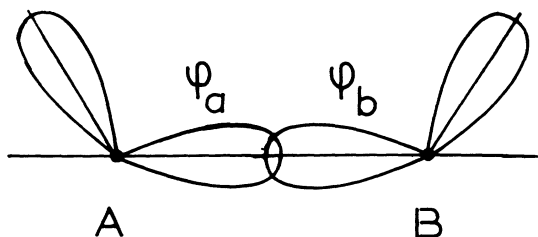


FIG. 1. Schematic representation of the atomic sp^3 hybrid orbitals in the bond AB .

E_A . The distance Δ between these two levels is given by

$$\Delta^2 = \left(\frac{2\beta^*}{1-S^2} \right)^2 + \left(\frac{\alpha_b - \alpha_a}{(1-S^2)^{1/2}} \right)^2, \quad (1.2)$$

where S stands for the overlap integral $\langle \varphi_a | \varphi_b \rangle$ and

$$\beta^* = \beta - S[(\alpha_a + \alpha_b)/2]. \quad (1.3)$$

Following equation (1.2), Δ can be divided into a homopolar term

$$E_h = \left| \frac{2\beta^*}{1-S^2} \right| \quad (1.4)$$

and a heteropolar term^{15,16}

$$C = \frac{\alpha_b - \alpha_a}{(1-S^2)^{1/2}}. \quad (1.5)$$

One can also define an ionicity parameter

$$F = \frac{C^2}{C^2 + E_h^2}. \quad (1.6)$$

We note that F corresponds to the square of the parameter f used in previous papers.^{15,16}

When further interactions are included, the molecular levels E_B and E_A widen into valence and conduction bands, respectively. Their barycenters are slightly shifted from E_B and E_A through the bonding-antibonding interactions. The corresponding effect is weak and could be treated by second-order perturbation theory. For the same reason, the charge density is mainly built from the bonding orbitals and, in the following, we shall take it as the superposition of the individual bond densities.

Let us then consider the bond of Fig. 1. If one writes the bonding orbital ψ_B as

$$\psi_B = C_a \varphi_a + C_b \varphi_b, \quad (1.7)$$

then its charge density is given by

$$\rho = 2(C_a^2 \varphi_a^2 + C_b^2 \varphi_b^2 + 2C_a C_b \varphi_a \varphi_b), \quad (1.8)$$

with:

$$C_a^2 = \frac{1}{2} \left[\frac{1-S(1-F)^{1/2}}{1-S^2} + \left(\frac{F}{1-S^2} \right)^{1/2} \right],$$

$$C_b^2 = \frac{1}{2} \left[\frac{1-S(1-F)^{1/2}}{1-S^2} - \left(\frac{F}{1-S^2} \right)^{1/2} \right],$$

$$2C_a C_b = \frac{1}{1-S^2} [(1-F)^{1/2} - S]. \quad (1.9)$$

The variations of these terms versus the ionicity parameter F are reported on Fig. 2.

A simple interpretation of Eq. (1.8) can be given. C_a^2 and C_b^2 correspond to the electronic charges on the atoms A and B and their difference describes a static charge transfer towards the atom A , which is proportional to $F^{1/2}$.^{15,16} The third term is a nonspherical part of the charge density and depends directly upon the overlap S of the atomic orbitals. One can easily show that this term, which cancels near the atoms, presents a maximum value along the bond. This maximum is located just at the middle of the bond for purely covalent crystals and is shifted towards the electronegative atoms for compounds. Then, it corresponds to the charge heaping up between the atoms, which is an important feature of the covalent bond. Integrating over the whole space, one can define a total overlap charge, or "bond charge,"

$$Q_S = \frac{2S}{1-S^2} [(1-F)^{1/2} - S], \quad (1.10)$$

the study of the variation of this charge with ionicity being of great interest in order to describe the chemical bonding in compound semiconductors.^{18,19} Particularly, one can note that Q_S vanishes for a critical value of the ionicity parameter:

$$F_C = 1 - S^2. \quad (1.11)$$

Then

$$C_a^2 = 1, \quad C_b^2 = 0, \quad (1.12)$$

the material becoming purely ionic.

The description of the ground-state wave func-

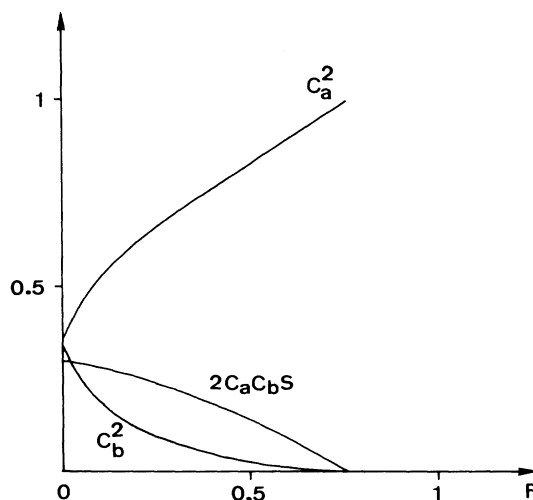


FIG. 2. Variations of the coefficients of Eq. (1.9) versus F . Values are computed with $S=0.5$.

TABLE I. Exponents of the Slater-type orbitals computed by Clementi *et al.*, Refs. 20 and 21: (1) *s* orbital and (2) *p* orbital.

	α_s (1)	α_p (2)		α_s (1)	α_p (2)
B	1.288	1.211	Ge	2.011	1.695
C	1.608	1.568	As	2.236	1.862
N	1.924	1.917	Se	2.439	2.072
Al	1.372	1.355	Cd	1.638	1.520
Si	1.634	1.428	In	1.902	1.694
P	1.881	1.629	Sn	2.126	1.820
Zn	1.491	1.467	Sb	2.322	1.999
Ga	1.767	1.555	Te	2.508	2.162

tion and, equivalently, of the electronic charge density requires the knowledge of the atomic orbitals φ_a and φ_b . We shall use here Slater-type orbitals. Optimal exponents for the free-atom functions have been derived by Clementi *et al.*^{20,21} from a variational calculation done in the Hartree-Fock approximation. Their values are reported in Table I. However, in order to test the accuracy of the wave functions obtained in this way, we have determined the F_{222} structure factor. For C, Si, and Ge we find 0.50, 0.72, and 0.78, which are lower than the experimental values 1.1, 1.5, and 1.1, respectively.²² To improve the agreement, it is necessary to contract the atomic orbitals, as is the case when atoms are placed into molecules.²³ A 15% increase of the exponents gives 0.83, 0.97, and 1.1, thus leading to a much more reasonable agreement. Details about this computation are given in Appendix A. So, from now on, we have assumed this particular increase for every material we consider. We shall see further that the results we obtain show little sensitivity to this parameter.

From these values, the overlap S can be computed. Using Clementi's exponents, values of order 0.65 are obtained while 15%-increased exponents lead to values nearly equal to 0.5, this last result also being quoted by Harrison.⁷ It is worth noticing that, for this second value of S , the critical ionicity defined by Eq. (1.11) is equal to 0.75 and is very near the one determined by Phillips, which is associated with the transition between fourfold and sixfold coordinated structures.¹⁷ Fol-

TABLE II. Cohesive energies E_c (Ref. 28); promotion energies e (Refs. 6 and 28). E_h is computed through equations (2.13) and (1.14). All values are in eV.

	E_c	e	E_h
C	7.3	2.1	16.1
Si	3.8	1.7	10.9
Ge	3.3	2.0	11.5
Sn	2.7	1.6	8.9

TABLE III. Ionicity parameters: (1) Phillips's scale, (2) our determination (see text).

	$F(1)$	$F(2)$
AIP	0.307	0.189
GaAs	0.310	0.122
ZnSe	0.676	0.369
InSb	0.321	0.168
CdTe	0.675	0.390

lowing Walter *et al.*¹⁸ this seems reasonable since, when F approaches F_c , electrostatic forces which hold atoms together in sixfold coordinated structures become more important than covalent forces which are dominant in fourfold coordinated structures. Nevertheless, a more precise comparison between these two critical ionicities would require a calculation of the cohesive energy with respect to F in the two structures.

The last parameter which is needed is the ionicity F . One can try to identify F with Phillips's ionicity, as in previous work¹⁶ where this has given good results for the transverse effective charges. However, there is no direct argument to prove this identification. So, it seems more appealing to determine F directly from Eq. (1.6), in view of the physical meaning of the parameters which are included. α_a and α_b can be evaluated semiempirically from free-atom values, taking the appropriate sp^3 average over s and p ionization potentials.¹⁶ For covalent systems, the integral β^* can be deduced from the cohesive energy. In the simple molecular model described above, one can easily show that this cohesive energy is given by

$$E = 4\beta^*/(1+S) - 4e, \quad (1.13)$$

e being the promotion energy needed to obtain the atoms in the sp^3 state. Knowing e from free-atom values and the experimental cohesive energies, β^* and then E_h are calculated through Eq. (1.13) (Table II). In the case of compounds, we retain the usual approximation²⁴ that E_h is equal to the value of the corresponding covalent system. The values of F computed in this way are given in Table III. They are substantially lower than Phillips's values but exhibit the same trends.

One can now try to compare these results with experiment or with previous calculations. First of all, the fact that the static electron transfer is towards the more electronegative atom, is in agreement with chemical-shift and x-ray measurements²⁵⁻²⁷ and, though quantitative comparison is not directly possible, correlations can easily be established between our values and experimental ones. Second, if one assumes that the bond charge can be equally divided between the atoms A and B , one can define atomic charges and compute the

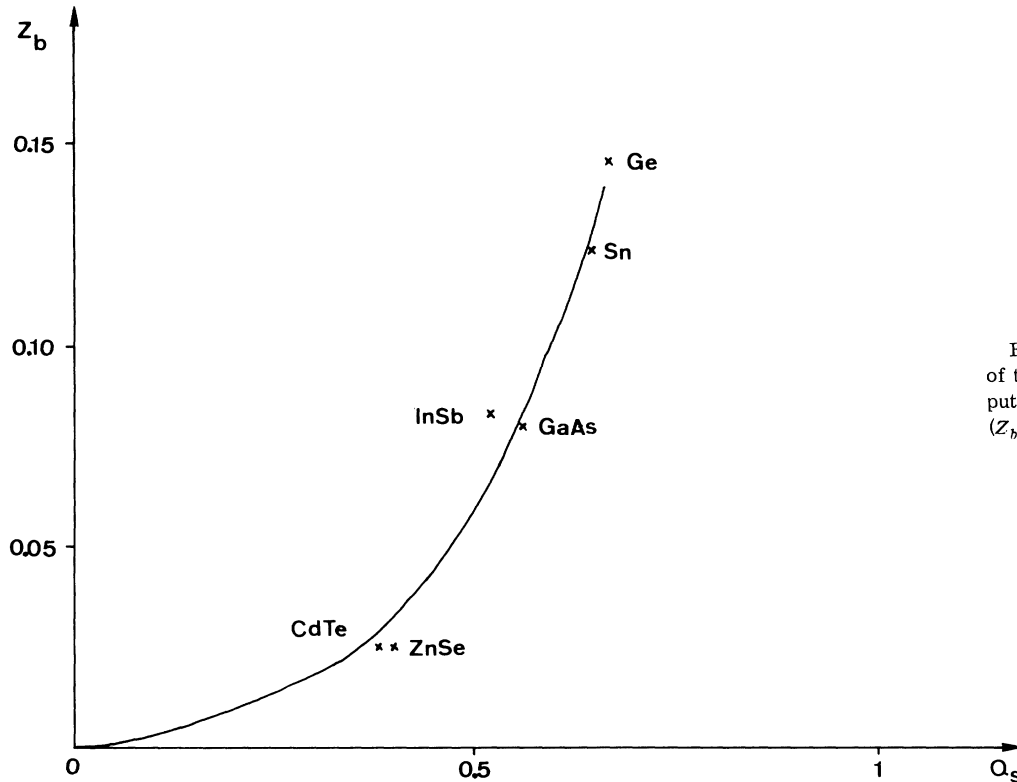


FIG. 3. Comparison of the bond charges computed by Walter *et al.* (Z_b) with ours (Q_s).

transverse effective charges following the method which has been developed previously.¹⁶ Here again, reasonable results are obtained. Finally one can compute from (1.10) the overlap charge and compare it to the results of recent calculations due to Walter *et al.*¹⁸ Although the two definitions of this charge are different, they should exhibit the same trends, when plotted versus the ionicity F , as is confirmed by Fig. 3. It is worth noticing here that this is not the case for the bond charges determined by Levine¹¹ from the assumption that they give the main contribution to the dielectric susceptibility. Their behavior is exactly opposite to the results of Fig. 3.

From all these facts, it appears that the molecular model described above is reasonable, and thus one can hope that it will give good results for all average properties of the valence electrons, when a detailed knowledge of the band structure is not required.²⁸ We shall then apply it to the computation of the static dielectric constant.

II. DIRECT COMPUTATION OF THE STATIC DIELECTRIC CONSTANT IN THE MOLECULAR MODEL

This section is concerned with the calculation of the static dielectric constant $\epsilon_1(0)$, in the molecular model described above, assuming that transitions from the bonding to antibonding states pre-

dominate. Such a model has been used by Phillips *et al.*⁴ and by Kleinman⁵ to determine higher-order dielectric susceptibilities in compound semiconductors. More recently, Harrison^{6,7} has deduced the static dielectric constant from a direct computation of the ground state in the presence of the electric field but we shall see farther that this procedure is rigorously equivalent to the model just mentioned. Let us now establish in detail the results of this model, in order to discuss the validity of the corresponding assumptions.

Using the well-known Kramers-Kronig relations, one can write

$$\epsilon_1(0) = 1 + \frac{2}{\pi} \int \frac{\epsilon_2(E')}{E'} dE' , \quad (2.1)$$

with, in the random-phase approximation,

$$\epsilon_2(E) = \frac{4\pi^2}{V} \sum_{v,c} \langle v | \xi | c \rangle \langle c | \xi | v \rangle \delta(E - (E_c - E_v)) . \quad (2.2)$$

$|v\rangle$ and $|c\rangle$ are two valence- and conduction-band states, E_v and E_c the corresponding energies, ξ the component of the electron position \vec{r} along the [111] axis, and V the crystal volume. Use is made of atomic units. In the molecular model, the valence- and conduction-band states are simply the bonding and antibonding states ψ_B and ψ_A , the difference between their energies being Δ . Thus

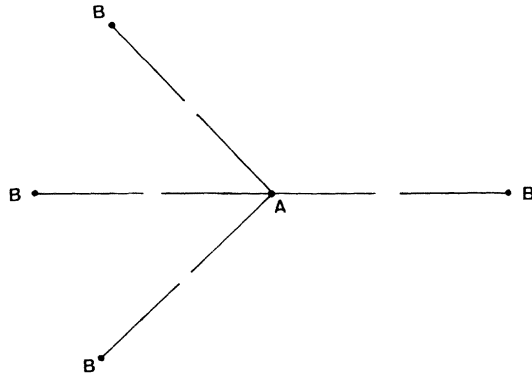


FIG. 4. Elementary cell.

$$\epsilon_1(0) = 1 + \frac{8\pi}{V\Delta} \sum_{i,j} |\langle B_i | \xi | A_j \rangle|^2, \quad (2.3)$$

the indices i and j running over every molecular orbitals of the crystal. $|B\rangle$ and $|A\rangle$ are given by

$$\begin{aligned} |B\rangle &= (1 + \lambda^2 + 2\lambda S)^{-1/2} (\varphi_a + \lambda \varphi_b), \\ |A\rangle &= (1 + \lambda'^2 - 2\lambda' S)^{-1/2} (\lambda' \varphi_a - \varphi_b), \end{aligned} \quad (2.4)$$

where

$$\lambda = C_b/C_a \quad (2.5)$$

and

$$\lambda' = (\lambda + S)/(1 + \lambda S) \quad (2.6)$$

to ensure the orthogonalization of the two eigenstates.

The sum in equation (2.3) can be reduced to the sum over the elementary cell represented on Fig. 4 in view of the translational invariance. Moreover, using the tetrahedral symmetry of the cell, one obtains

$$\epsilon_1(0) = 1 + \frac{4\pi\sqrt{3}}{R^3\Delta} \sum_j |\langle B | \vec{r} | A_j \rangle|^2, \quad (2.7)$$

where $|B\rangle$ is any one of the four bonding orbitals in the cell, R is the nearest-neighbor distance, and the spin degeneracy has been taken into account.

An important test of the accuracy of this model is provided by the verification of the f -sum rule:

$$\frac{2}{\pi} \int E \epsilon_2(E) dE = \omega_p^2, \quad (2.8)$$

where ω_p is the plasma frequency. With the help of the above results, this leads to

$$\frac{2}{3} \Delta \sum_j |\langle B | \vec{r} | A_j \rangle|^2 = 1, \quad (2.9)$$

the first member of this equation requiring the same computation as for $\epsilon_1(0)$.

First of all, we shall look at a simple limit of the molecular model, showing that the above formulation includes Harrison's one. We assume

that the spatial extension of the atomic orbitals is negligible with respect to nearest-neighbor distance. Then, the interatomic matrix elements, and thus the overlap integral S , become negligible and one obtains

$$\sum_j |\langle B | \vec{r} | A_j \rangle|^2 = \left(\frac{\lambda R}{1 + \lambda^2} \right)^2, \quad (2.10)$$

where

$$\lambda = (1 - F^{1/2})/(1 + F^{1/2}). \quad (2.11)$$

Thus

$$\epsilon_1(0) = 1 + \frac{\pi\sqrt{3}}{R} \frac{E_h^2}{(E_h^2 + C^2)^{3/2}}. \quad (2.12)$$

Apart from a scaling parameter which does not enter directly into the model, this is identical to Harrison's result. Moreover, the f -sum rule, in the form of Eq. (2.9), becomes

$$\frac{2\Delta}{3} \left(\frac{\lambda R}{1 + \lambda^2} \right)^2 = 1. \quad (2.13)$$

This relation surely fails when λ approaches zero, i. e. for the more ionic compounds. This point can easily be understood by noticing that, in this limit, one obtains

$$\psi_B = \varphi_a, \quad \psi_A = \varphi_b. \quad (2.14)$$

As interatomic terms have been neglected, this means that, in the more ionic materials, the main part of the oscillator strength is due to intra-atomic terms which have not been included.

It is now interesting to determine the influence of the spatial extension of the atomic orbitals. For this, we have used the Slater-type orbitals with the exponents discussed in Sec. I, and we have considered every transition from the bonding state of a molecular orbital to the antibonding states of the same orbital and of the adjacent orbitals. For the parameter Δ , we have used the set of values discussed in Sec. I. In Table IV, results are given for the purely covalent materials. One can note that the sum rule is not exactly satisfied, particularly for C. On Fig. 5, results have been plotted against the bond parameter λ for two compounds. Here again, when λ approaches zero, the f sum becomes very weak.

In view of these results, one can first conclude that the use of the f -sum rule to determine the matrix elements which are needed in the computation

TABLE IV. f sum under the form of Eq. (2.9).

C	0.475
Si	0.725
Ge	0.820
Sn	0.815

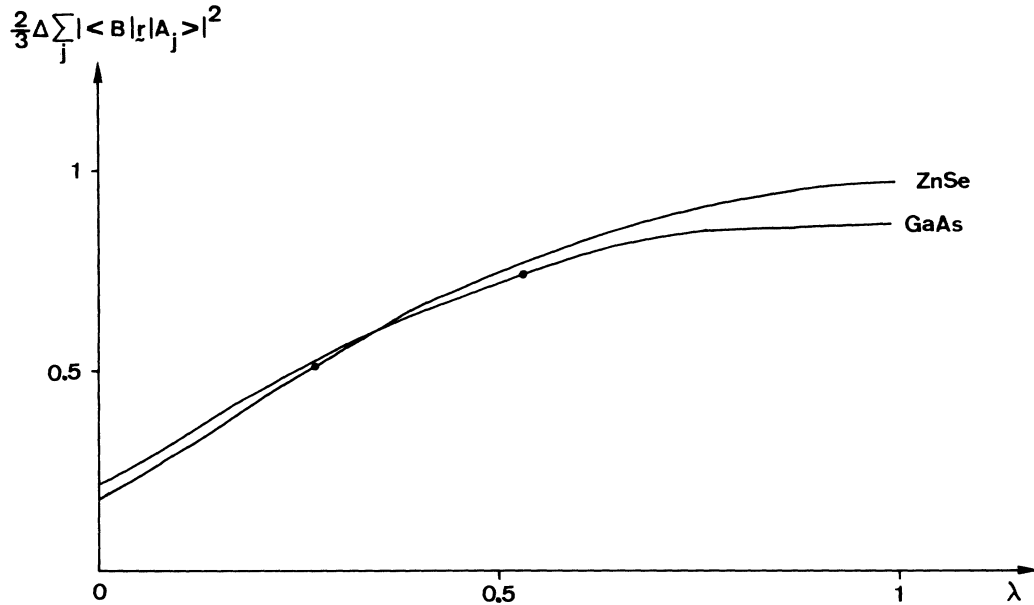


FIG. 5. Variation of the f sum computed under the form of Eq. (2.9) versus the bond parameter λ . Dots indicate the results for the ionicity values computed in Sec. I.

of the susceptibilities is incorrect, particularly for the more ionic compounds. However, the direct computation of $\epsilon_1(0)$ within this model depends upon the moment of order -1 of $\epsilon_2(E)$ while the f sum is associated with the moment of order 1. Thus, the weights of the various states are not the same in the two computations, and conclusions about the f sum are not directly applicable to $\epsilon_1(0)$. Nevertheless, one can note that the variations of the f sum when going from purely covalent materials, such as Ge, to ionic materials, such as ZnSe, is very large, and thus the dependence of $\epsilon_1(0)$ on ionicity can be completely hidden by this effect. So, the bond-orbital model parameters which are deduced from the above approximations are probably less correct for the more ionic materials. This casts some doubt on the $\frac{3}{2}$ exponent occurring in the denominator of Eq. (2.12), which was considered by Harrison as being an important feature of the behavior of $\epsilon_1(0)$ as a function of the heteropolar term C .

We then believe that a model which describes electric field effects uniquely in terms of transitions from bonding to antibonding molecular states cannot give accurate predictions concerning the dielectric susceptibilities of the more ionic compounds, and that any agreement with experiment should be considered as fortuitous. Any quantitative model should incorporate transitions which complete the f -sum rule in the ionic limit. This will be the aim of Sec. III, with the help of a method of moments.

III. CALCULATION OF $\epsilon_1(0)$ IN TERMS OF THE MOMENTS OF $\epsilon_2(E)$

One can define the moments M_n of $\epsilon_2(E)$ through the relation

$$M_n = \frac{2}{\pi} \int \epsilon_2(E) E^n dE . \quad (3.1)$$

Then, Eq. (2.1) can be rewritten

$$\epsilon_1(0) = 1 + M_{-1} . \quad (3.2)$$

The knowledge of the moment of order -1 of the $\epsilon_2(E)$ curve gives directly the static dielectric constant. Unfortunately, this curve cannot be computed in the molecular model described above, but one can determine a finite set of moments M_0, M_1, M_2, \dots , which, though they do not suffice to reconstruct the entire curve, provide interesting information about it and can lead to reasonable results for $\epsilon_1(0)$. For this, we shall derive expressions of these moments, which only require the knowledge of the ground-state wave function, and show that $\epsilon_1(0)$ can be written in the form used by Phillips in the spectroscopic model.¹⁷ This will allow a direct determination of the average energy gap E_g .

Starting with the Eq. (2.2) and using the closure relation, one obtains²⁹

$$M_n = \frac{8\pi}{V} \sum_v \left(\langle v | \xi [n] | v \rangle - \sum_{v'} \langle v | \xi | v' \rangle \langle v' | [n] | v \rangle \right) , \quad (3.3)$$

where v and v' stand for valence-band states and

$$[n] = [H, [H, [H, \dots [H, \xi]]]] . \quad (3.4)$$

Applying these results, one can compute the lowest-order moments:

$$M_0 = \frac{8\pi}{V} \sum_v \left(\langle v | \xi^2 | v \rangle - \sum_{v'} \langle v | \xi | v' \rangle \langle v' | \xi | v \rangle \right) , \quad (3.5)$$

$$M_1 = \omega_p^2 , \quad (3.6)$$

$$M_2 = \frac{8\pi}{V} \sum_v \left(\langle v | p_x^2 | v \rangle - \sum_{v'} \langle v | p_x | v' \rangle \langle v' | p_x | v \rangle \right), \quad (3.7)$$

where ω_p is the plasma frequency and p_x the x component of the momentum operator. Equation (3.6) is in fact a statement of the f -sum rule.

For $n > 2$, the calculation of M_n involves the potential and its successive derivatives. Developing the expression of the third moment, for instance, one can easily demonstrate, within this formalism, the Hopfield sum rule,³⁰ which relates M_3 to the product of the electron density fluctuations and the Laplacian of the crystal potential.

For $n > 3$, one has to take care of the asymptotic behavior of $\epsilon_2(E)$ in the high-energy range. $\epsilon_2(E)$ tends to zero according to a power law, which leads to divergences in the higher-order moments. This law can easily be established if one computes directly the contribution of the transitions from the valence states to the high-energy free electron states (Appendix B). Denoting the radial part of the atomic orbitals from which valence states are built up by the form

$$\psi(r) = N r^{p-1} e^{-\alpha r}, \quad (3.8)$$

one obtains

$$\epsilon_2(E) \propto E^{-p-5/2} \quad (3.9)$$

if p is even, and

$$\epsilon_2(E) \propto E^{-p-7/2} \quad (3.10)$$

if p is odd.

It is worth noticing that, in the special case of transitions from the $1s$ states, Kabir and Salpeter³¹ and Rau and Fano³² have obtained an exponent equal to $-\frac{9}{2}$, corresponding to $n=1$ in the above results. In view of these rates of decrease, M_n will diverge from M_4 for C, M_6 for Si and Ge, and M_8 for Sn, when use is made of Slater-type orbitals. This result is confirmed by a direct computation of the moments through Eq. (3.3). This point is particularly interesting and will be discussed further, to develop a model for $\epsilon_2(E)$.

Coming back to the static dielectric constant one can write

$$\epsilon_1(0) = 1 + \omega_p^2 / E_g^2, \quad (3.11)$$

where:

$$E_g^2 = M_1 / M_{-1}. \quad (3.12)$$

This is the form derived by Phillips, in the spectroscopic model, and Eq. (3.12) allows the computation of the average dielectric gap E_g .¹⁷ However, the expressions given above take into account all transitions from the valence-band states, namely, transitions toward the inner states which do not contribute to the susceptibility, since these states are occupied. This point is in general not serious,

except for d states which are closer to the valence band than others, but corrections due to these states are included in Phillips's determination of E_g , to which we shall compare our results.

The computation of M_{-1} , knowing the first moments M_0 , M_1 , and M_2 , is a problem which has previously been resolved for the calculation of various integral properties of the electron density of states.³³⁻³⁵ We shall follow a similar method and represent $\epsilon_2(E)$ in an approximate way, such as, within the model, the first moments of the approximate curve be equal to the exact ones. First of all, one can replace $\epsilon_2(E)$ by a δ function at an unknown energy E_1 . Denoting

$$m_n = M_n / M_0, \quad (3.13)$$

one obtains

$$E_g = m_1. \quad (3.14)$$

In this case, the whole method described above is equivalent to the two-parameter variational procedure used by Flytzanis and Ducuing, i. e., the Unsöld approximation.¹⁰

Then, one can develop a second model which takes account of the width of the $\epsilon_2(E)$ curves and one can build up this model from the power law given by Eqs. (3.9) and (3.10). Moreover, an important feature appears in the low-energy range of the experimental spectra, namely, a threshold energy under which no transition occurs. This can be included in the $\epsilon_2(E)$ model curve through a low-energy cutoff.³⁶ In order to take account of these two points, use has been made of the function

$$\begin{aligned} \epsilon_2(E) &= 0 & \text{if } E < E_0, \\ \epsilon_2(E) &= A(E - E_1)^{-m} & \text{if } E \geq E_0, \end{aligned} \quad (3.15)$$

where $m = p + \frac{5}{2}$ or $m = p + \frac{7}{2}$ according to the parity of p .

The parameters E_0 and E_1 , and then the average gap E_g , can be determined from the reduced moments m_1 and m_2 . Results are plotted on Fig. 6.

In Sec. IV, these two models will be discussed, through the comparison of our values of E_g with Phillips's values. But, it is worth noticing that the second model introduces a new interesting parameter, i. e., the threshold energy E_0 , which can also be compared with experimental values.

IV. CALCULATION OF THE AVERAGE DIELECTRIC GAP E_g IN THE MOLECULAR MODEL; DISCUSSION

Using Eq. (3.5) one can write M_0 in the molecular model:

$$M_0 = \frac{2\pi N}{V} \sum_i \left(\langle B_i | \xi^2 | B_i \rangle - \sum_j |\langle B_i | \xi | B_j \rangle|^2 \right), \quad (4.1)$$

where N and V , respectively, stand for the total number of electrons and the whole crystal volume,

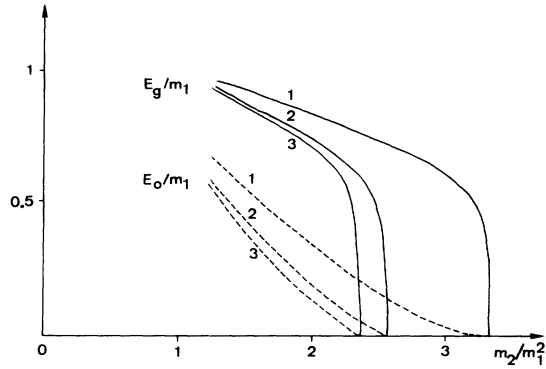


FIG. 6. Variations of the threshold energy E_0 and the average gap E_g , normalized to m_1 , with the ratio m_2/m_1^2 . Plots are given for the various power laws: 1, C; 2, Si and Ge; 3, Sn.

the sum runs over the molecular bonds of the elementary cell represented on Fig. 4, and $|B_i\rangle$ and $|B_j\rangle$ are given by Eq. (2.4). In the same way

$$M_2 = \frac{2\pi N}{V} \sum_i \left(\langle B_i | p_i^2 | B_i \rangle - \sum_j |\langle B_i | p_i | B_j \rangle|^2 \right). \quad (4.2)$$

Following the procedure described in Sec. II, one obtains

$$M_0 = \frac{8\pi N}{3V} \left(\langle B | r^2 | B \rangle - \sum_j |\langle B | \vec{r} | B_j \rangle|^2 \right), \quad (4.3)$$

$$M_2 = \frac{8\pi N}{3V} \left(\langle B | p^2 | B \rangle - \sum_j |\langle B | \vec{p} | B_j \rangle|^2 \right),$$

where $|B\rangle$ is any one of the four bonding orbitals in the elementary cell. Every matrix element between a bonding orbital and either itself or the adjacent bonding orbitals has been considered. Computation has been done using Slater-type orbitals with the exponents discussed in Sec. I. Results are given in Table V for purely covalent materials, and they are plotted against the bond parameter λ for two compounds on Fig. 7.

First of all, one can discuss the validity of the second model. On Fig. 8, theoretical curves are compared to experimental results^{37,38} for C, Si, and Ge. A reasonable agreement is obtained in the high-energy range, as well as for the thresh-

TABLE V. Average dielectric gap E_g (1) within the one- δ -function model, (2) within the second model (see text), and (3) Phillips's values (Ref. 17). Low-energy cutoff E_0 of the second model. All energies are in eV.

	E_g (1)	E_g (2)	E_g (3)	E_0
C	20.0	17.9	13.6	10.2
Si	9.1	7.7	4.8	3.4
Ge	8.3	7.0	4.3	3.2
Sn	6.5	5.2	3.1	2.0

old energy. This second point is very interesting, if one remembers that the above computations only require a simple LCAO description of the ground state, rather than a detailed knowledge of the band structure, particularly of the conduction band, and thus, it gives us confidence in this model. Nevertheless, the theoretical curves cannot exhibit the structures of the experimental curves in the low-energy range. One has to note that this is also the case for the constant-conductivity model developed by Wemple *et al.*³⁶ as well as for recent results obtained by Breckenridge *et al.*³⁹ within the Penn model [Fig. 8(b)]. The contributions of these structures will be discussed farther. In the case of compounds, the same agreement is obtained for E_0 , as shown on Fig. 7.

Before discussing the results we have obtained for E_g , we shall treat two particular points. First of all, we have looked at the influence of the values of the screening constants. The reduced moments m_1 and m_2 , and thus the threshold energy E_0 and the average gap E_g , are only slightly sensi-

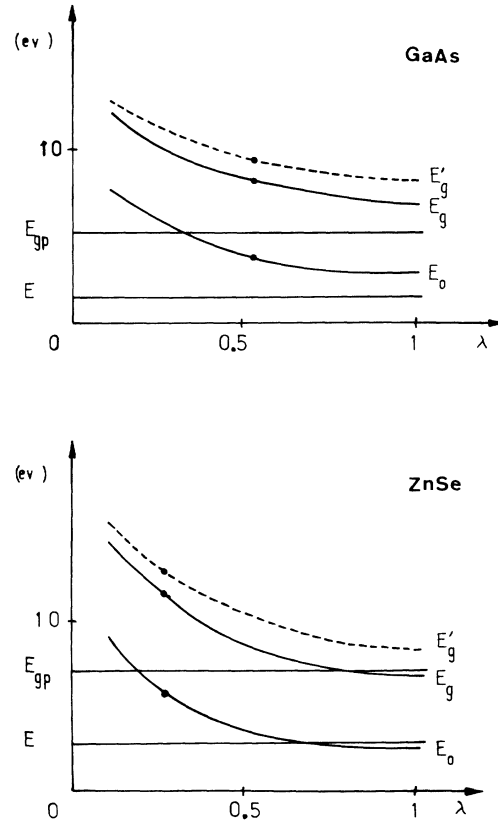


FIG. 7. Variations of the threshold energy E_0 and the average gap E_g versus the bond parameter λ . Variation of E_g' computed within the one- δ -function model is also reported. Horizontal lines correspond to Phillips's results (E_{gp}) and to the experimental threshold energies, Ref. 24 (E).

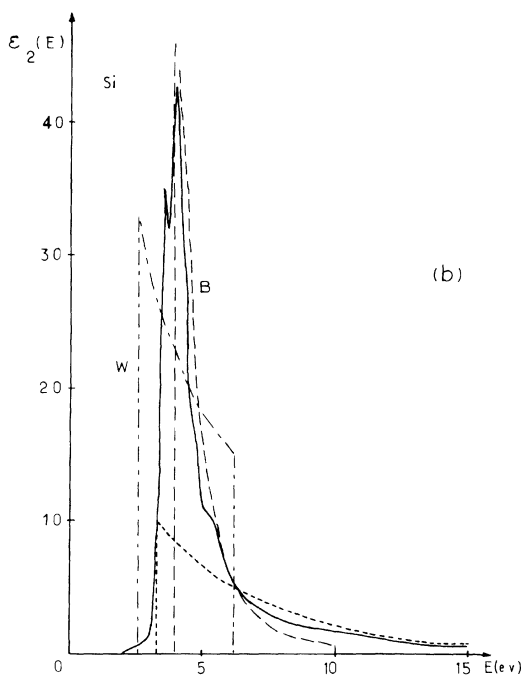
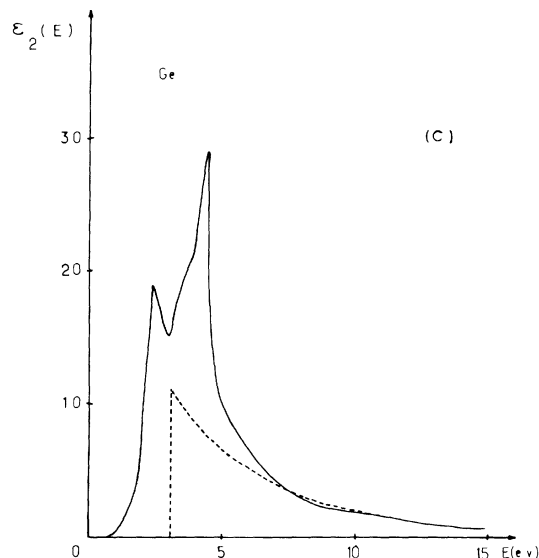
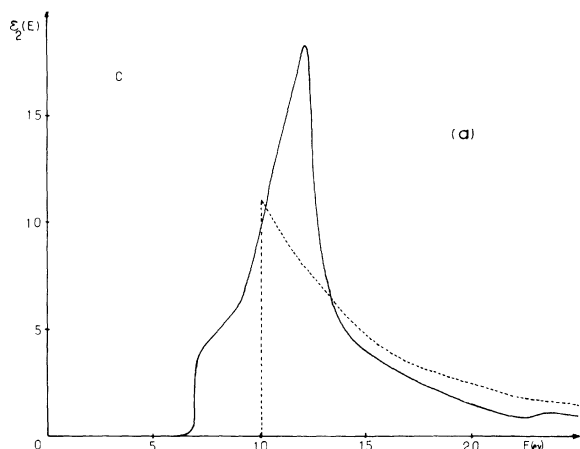


FIG. 8. Comparison of the experimental (full line) and theoretical (dashed line) curves for $\epsilon_2(E)$: (a) diamond; (b) silicon; (c) germanium. In the case of Si (b), results of Wemple *et al.*, Ref. 36 (W) and Breckenridge *et al.*, Ref. 39 (B) are also reported.

to a less extent E_g will be decreased (Fig. 6). Since this effect is not included in the computation of m_1 and m_2 , it seems to us better to use $-\frac{13}{2}$ and $-\frac{17}{2}$ for Si, Ge, and Sn.

Now, one can compare the average dielectric gaps E_g we have obtained with those of Phillips. Results have been reported on Fig. 9. Though our values are too large, a strong correlation appears in the case of purely covalent materials, since the dependence is nearly linear. One can note that this difference between the values of E_g can be associated with the difference between the theoretical and experimental curves of $\epsilon_2(E)$ in the low-energy range, since the weight of the low-energy states is important in the moment of order -1 . The linear law mentioned above is roughly followed by the compounds when use is made of the ionicity parameters given in Sec. I. It is interesting to note that this is not the case if Phillips's ionicity is used and thus the inclusion of this scale within a molecular model can be questionable.

The fact that the values of E_g we obtain are too large can be explained by the local-field correction, as has previously been emphasized for compounds by Flytzanis *et al.*,¹⁰ and it seems that the same argument can be developed, at least partially, for the $\epsilon_2(E)$ spectra, as mentioned by Lubinsky *et al.*⁴⁰ Direct computations of this correction have been done recently⁴¹⁻⁴³ but they lead to different results and thus do not establish its influence in a definitive way. However, it has been proved by Wisner¹³ and more recently by Sinha *et al.*⁴⁴ that,

tive to variations of these values, which have no influence on the previous conclusions. Second, we have to come back to the power law followed by the high-energy tail of the $\epsilon_2(E)$ spectra. In fact, a more correct description of the bonding wave function requires the orthogonalization of the Slater-type orbitals to core-state orbitals. Then this bonding wave function possesses a $1s$ component and, according to Eq. (3.10), it seems that the rate of decrease of $\epsilon_2(E)$ could be described better by a $-\frac{3}{2}$ power law. Nevertheless, one has to keep in mind that core-state components will also be included in the computation of m_1 and m_2 . In fact, only m_2 is increased by the orthogonalization procedure, since it depends upon matrix elements of p^2 and \vec{p} , which are greater for the core states than for the valence states, and thus E_0 and

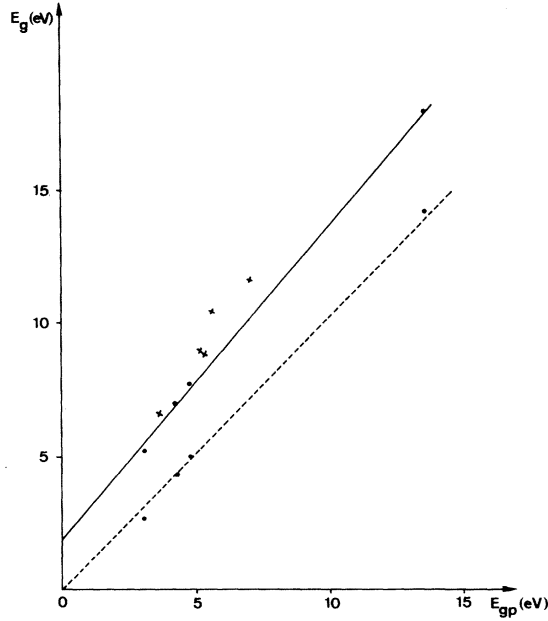


FIG. 9. Comparison of E_g and E_{gp} . Full line: local-field correction neglected; dashed line: local-field correction included. Dots correspond to purely covalent materials while crosses correspond to compounds.

in the tight-binding limit used here, a Lorentz-Lorenz-type correction is available. In this case

$$\epsilon_1(0) = 1 + \frac{4\pi\alpha}{1 - \frac{4}{3}\pi\alpha}, \quad (4.4)$$

where α is the polarizability of the elementary cell. Denoting

$$\alpha = \alpha_0 - \alpha_{sp}, \quad (4.5)$$

where α_0 is the polarizability computed above and α_{sp} the self-polarization term,¹³ one can easily write down Eq. (4.4) in the form

$$\epsilon_1(0) = 1 + \frac{(\omega_p/E_g)^2}{1 - (\frac{1}{3} - \theta)(\omega_p/E_g)^2}, \quad (4.6)$$

where θ is directly related to α_{sp} . This relation can be demonstrated within the bonding-antibonding model, and preliminary calculations have allowed us to show that θ is roughly constant for the purely covalent materials.⁴⁵ Thus, if one writes

$$\epsilon_1(0) = 1 + (\omega_p/E_{gp})^2, \quad (4.7)$$

where E_{gp} is Phillips's average dielectric gap, one should obtain simply

$$E_g^2 = E_{gp}^2 + (\frac{1}{3} - \theta)\omega_p^2, \quad (4.8)$$

which approximately leads to

$$E_g = E_{gp} + (\frac{1}{3} - \theta)\omega_p^2/2E_{gp} \quad (4.9)$$

if the second term of Eq. (4.8) is smaller than E_{gp} . As ω_p^2/E_{gp} is a slowly varying function of E_{gp} ,

Eq. (4.9) is a linear law of slope 1 which is in reasonable agreement with the results of Fig. 9. Moreover, Eq. (4.8) provides a determination of θ , which is obtained equal to 0.21. In order to test the validity of this result, the values of E_g corrected for the local-field effect have been plotted against Phillips's values on Fig. 9, showing a correct agreement. Then, one can conclude that within a tight-binding limit, the Lorentz-Lorenz correction remains available for purely covalent materials if one takes account of the drastic reduction due to the self-polarization effect. In the case of compounds, values of E_g corrected in the same way have been reported in Table VI. It seems that, in this case, the value of θ must be reduced, thus increasing the local-field correction with respect to the covalent case. Work to justify this point is in progress.⁴⁵ However it is not possible to detail here the corresponding arguments.

We believe from this study that the method of moments gives a coherent picture of $\epsilon_2(E)$ and $\epsilon_1(0)$. It provides a reasonable estimate of the threshold energy E_0 occurring in $\epsilon_2(E)$. It is then likely that it leads to a correct order of magnitude of E_g . The difference with the experimental values must then be attributed to a local-field correction, including self-polarizability effects. At last, one can note that the one- δ -function model which leads to values of E_g greater than those of the second model, but not too different (Table V and Fig. 7), appears interesting in view of its simplicity, and thus it seems well suited for more complex problems, such as the computation of higher-order susceptibilities.¹⁰

A final point can be made concerning the validity of the bond-charge model¹¹ or charge-transfer model.¹² At each stage of the above computations, the contributions of intra-atomic and interatomic terms to the static dielectric constant can be separated and one can show that they are of the same order. As these terms can be associated with charge-transfer and bond-charge contributions, it seems to us that none of them can be neglected, and, though this conclusion is not directly applicable to second-order susceptibility, we think that it remains roughly valid.

TABLE VI. (1) Value of E_g corrected for local-field effect (see text), and (2) Phillips's values (Ref. 17). All energies are in eV.

	E_g (1)	E_{gp} (2)
AlP	8.7	5.6
GaAs	5.9	5.2
ZnSe	10.3	7.1
InSb	4.7	3.7
CdTe	7.7	5.4

CONCLUSION

Though theoretical models have given interesting informations about the origins of the nonlinear dielectric susceptibilities, they were often built on a more-or-less justified basis. The parameters used in these calculations were generally determined in order to give the experimental values of the static dielectric constant $\epsilon_1(0)$. In this work, we have computed directly $\epsilon_1(0)$ within a molecular model. This has allowed us to discuss the different approximations, as well as to estimate the local-field corrections.

First of all, we have shown that the direct calculation of $\epsilon_1(0)$ in terms of transitions between bonding and antibonding molecular states does not verify the f -sum rule, particularly for the most ionic compounds. Thus, it appears that models using this description are questionable.

Then, $\epsilon_1(0)$ has been computed with the help of a method of moments. Model curves for $\epsilon_2(E)$ have been determined, such as their first moments being equal to the exact moments, and then the average dielectric gap E_g defined by Phillips has been directly calculated. The most interesting model, which takes account of the essential features of $\epsilon_2(E)$ in the high- and low-energy ranges, allows the determination of the low-energy threshold of the $\epsilon_2(E)$ spectrum, starting with a simple LCAO description of the ground state. Reasonable agreement with experimental values has been obtained. Values of E_g , though strongly correlated with Phillips's values, were too large, but the inclusion of local-field effects has led to satisfactory results. We have shown that a Lorentz-Lorenz correction is available if self-polarization effects are included. Finally, we have noted that intra-atomic and inter-atomic terms, within the expressions of the moments which are used, are of the same order. Thus, it appears that neither the contribution of the charge transfer, nor that of the bond charge can be neglected.

It seems to us that the application of this model to the computation of the nonlinear susceptibilities can give interesting and valid informations as well for the computations of other properties, such as magnetic susceptibilities,⁴⁶ which are directly related to the moments of the electron distribution. Moreover, this model can give important features of the $\epsilon_2(E)$ spectrum of other semiconductors, such as Se and Te, without requiring a detailed knowledge of their band structure. At last, it can be a new tool to obtain simple informations about the local-field effects.

APPENDIX A

The determination of the F_{222} structure factor requires the computation of the integral

$$F = \int \rho e^{i\vec{k}\cdot\vec{r}} d\tau, \quad (\text{A1})$$

where ρ is given by Eq. (1.8) and \vec{K} is the vector $(2\pi/a)(2, 2, 2)$, a being the lattice parameter. According to the symmetry of the crystals we consider the contributions of terms which are centered on the atomic sites vanish, and thus, in the case of covalent materials, the integral reduces to

$$F = \frac{2}{1+S} \int \varphi_a \varphi_b e^{i\vec{k}\cdot\vec{r}} d\tau. \quad (\text{A2})$$

Moreover, in view of the form of the product $\varphi_a \varphi_b$, it can be simply described by a Gaussian distribution of the electron density along each bond. Then, one can write

$$\varphi_a \varphi_b = A e^{-\nu r^2}, \quad (\text{A3})$$

the origin of the electron coordinate \vec{r} being taken at the middle of the bond. In order to determine the parameters A and ν , one can assume that the moments of order 0 and 2 of this Gaussian distribution are equal to the corresponding moments of the exact distribution:

$$\int \varphi_a \varphi_b d\tau = A \int e^{-\nu r^2} d\tau \quad (\text{A4})$$

and

$$\int \varphi_a \varphi_b r^2 d\tau = A \int e^{-\nu r^2} r^2 d\tau. \quad (\text{A5})$$

The first integral is just the overlap S . Then, knowing A and ν , F is easily computed. One obtains

$$F = \frac{2S}{1+S} e^{-K^2 \langle r^2 \rangle / 6S}, \quad (\text{A6})$$

where $\langle r^2 \rangle$ stands for the integral (A5). If the structure factor is computed per cubic cell,

$$F_{222} = 16F. \quad (\text{A7})$$

Numerical values are discussed in Sec. I.

APPENDIX B

The contribution to $\epsilon_2(E)$ of transitions from valence states to high-energy free-electron states can be written

$$\epsilon_2(E) \propto \sum_{\vec{k}} \left| \int \varphi(\vec{r}) \vec{r} e^{i\vec{k}\cdot\vec{r}} d\tau \right|^2 \delta(E - (E_{\vec{k}} - E_v)), \quad (\text{B1})$$

where $\varphi(\vec{r})$ is given by Eq. (3.8) and E_v is the bonding-state energy. In the high-energy range, E_v can be neglected with respect to $E_{\vec{k}}$. The integration of the angular part giving, for large values of k , a contribution of the type

$$\cos k r / k r, \quad (\text{B2})$$

the integral which appears in Eq. (B1) can easily be written,

$$I \propto \int_0^{\infty} r^{p+1} e^{-\alpha r} (e^{ikr} + e^{-ikr}) dr, \quad (\text{B3})$$

which gives

$$I \propto \frac{1}{k} \frac{(\alpha + ik)^{p+2} + (\alpha - ik)^{p+2}}{(\alpha^2 + k^2)^{p+2}}. \quad (\text{B4})$$

Then, if p is even

$$I \propto 1/k^{p+3}, \quad (\text{B5})$$

while if p is odd

$$I \propto 1/k^{p+4}, \quad (\text{B6})$$

and one obtains

$$\epsilon_2(E) \propto \sum_{\mathbf{k}} \delta(E - E_{\mathbf{k}}) k^{-m}, \quad (\text{B7})$$

where m equals $2p+6$ or $2p+8$ following p being even or odd. Then, denoting

$$E = K^2/2, \quad (\text{B8})$$

the relation

$$\delta(E - E_{\mathbf{k}}) = (1/k) \delta(k - K) \quad (\text{B9})$$

leads to

$$\epsilon_2(E) \propto \int k^{-m-1} \delta(k - K) k^2 dk \quad (\text{B10})$$

and

$$\epsilon(E) \propto E^{-[(m-1)/2]}, \quad (\text{B11})$$

which gives directly Eqs. (3.9) and (3.10).

*Equipe de recherche associée au CNRS.

¹S. L. Adler, Phys. Rev. **126**, 413 (1962).

²J. A. Armstrong, N. Bloembergen, J. Ducuing, and P. S. Pershan, Phys. Rev. **127**, 1918 (1962).

³P. L. Kelley, J. Phys. Chem. Solids **24**, 607 (1963).

⁴J. C. Phillips and J. A. Van Vechten, Phys. Rev. **183**, 709 (1969).

⁵D. A. Kleinman, Phys. Rev. B **2**, 3139 (1970).

⁶W. A. Harrison, Phys. Rev. B **8**, 4487 (1973).

⁷W. A. Harrison and S. Ciraci, Phys. Rev. B **10**, 1516 (1974).

⁸F. N. H. Robinson, Bell Syst. Tech. J. **46**, 913 (1967).

⁹S. Jha and N. Bloembergen, Phys. Rev. **171**, 891 (1968).

¹⁰Chr. Flytzanis and J. Ducuing, Phys. Rev. **178**, 1218 (1969).

¹¹B. F. Levine, Phys. Rev. B **7**, 2600 (1973).

¹²C. L. Tang and Chr. Flytzanis, Phys. Rev. B **4**, 2520 (1971).

¹³N. Wisser, Phys. Rev. **129**, 62 (1963).

¹⁴C. A. Coulson, L. B. Redei, and D. Stocker, Proc. R. Soc. Lond. **270**, 352 (1962).

¹⁵J. N. Decarpigny and M. Lannoo, J. Phys. (Paris) **34**, 651 (1973).

¹⁶M. Lannoo and J. N. Decarpigny, Phys. Rev. B **8**, 5704 (1973).

¹⁷J. C. Phillips, Rev. Mod. Phys. **42**, 317 (1970).

¹⁸J. P. Walter, and M. L. Cohen, Phys. Rev. B **4**, 1877 (1971).

¹⁹C. M. Bertoni, V. Bortoloni, C. Calandra, and F. Nizzoli, J. Phys. C **6**, 3612 (1973).

²⁰E. Clementi and D. L. Raimondi, J. Chem. Phys. **38**, 2686 (1963).

²¹E. Clementi, D. L. Raimondi, and W. P. Reinhardt, J. Chem. Phys. **47**, 1300 (1967).

²²J. P. Lelieur and G. Leman, J. Phys. (Paris) **27**, 549 (1966).

²³J. C. Slater, *Quantum Theory of Molecules and Solids* (McGraw-Hill, New York, 1963), Vol. 1.

²⁴M. L. Cohen and T. K. Bergstresser, Phys. Rev. **141**, 789 (1966).

²⁵G. Leonhardt, A. Berndtsson, J. Hedman, M. Klasson, R. Nilsson, and C. Nordling, Phys. Status Solidi B **60**, 241 (1973).

²⁶N. J. Shevchik, J. Tejada, and M. Cardona, Phys. Rev. B **9**, 2627 (1974).

²⁷R. J. Weiss, Philos. Mag. **29**, 1029 (1974).

²⁸G. Leman and J. Friedel, J. Appl. Phys. Suppl. **33**, 281 (1962).

²⁹M. Lannoo and J. N. Decarpigny, J. Phys. (Paris) **35**, C3-97 (1974).

³⁰J. J. Hopfield, Phys. Rev. B **2**, 973 (1970).

³¹P. K. Kabir and E. E. Salpeter, Phys. Rev. **108**, 1256 (1957).

³²A. R. P. Rau and U. Fano, Phys. Rev. **162**, 68 (1967).

³³F. Cyrot-Lackmann, Adv. Phys. **16**, 393 (1968).

³⁴F. Cyrot-Lackmann, J. Phys. Chem. Solids **29**, 1235 (1968).

³⁵M. Lannoo and P. Lenglard, J. Phys. (Paris) **32**, 427 (1971).

³⁶S. H. Wemple and M. Didomenico, Jr., Phys. Rev. B **3**, 1338 (1971).

³⁷H. R. Philipp and H. Ehrenreich, Phys. Rev. **129**, 1550 (1963).

³⁸H. R. Philipp and E. A. Taft, Phys. Rev. **136**, A1445 (1964).

³⁹R. A. Breckenridge, R. W. Shaw, Jr., and A. Sher, Phys. Rev. B **10**, 2483 (1974).

⁴⁰A. R. Lubinsky, D. E. Ellis, and G. S. Painter, Phys. Rev. B **6**, 3950 (1972).

⁴¹J. A. Van Vechten and R. M. Martin, Phys. Rev. Lett. **28**, 446 (1972).

⁴²W. Hanke and L. J. Sham, Phys. Rev. Lett. **33**, 582 (1974).

⁴³S. G. Louie, J. R. Chelikowsky, and M. L. Cohen, Phys. Rev. Lett. **34**, 155 (1975).

⁴⁴S. K. Sinha, R. P. Gupta, and D. L. Price, Phys. Rev. B **9**, 2564 (1974).

⁴⁵A detailed description of this work is being prepared for publication.

⁴⁶R. M. White, Phys. Rev. B **10**, 3426 (1974).